



# An analytical method for estimating leakage from a hydraulic pressure tunnel

Yong Huang<sup>1</sup> · Huiyang Qiu<sup>1</sup> · Zhi Dou<sup>1</sup> · Zhimin Fu<sup>2</sup> · Zhifang Zhou<sup>1</sup>

Received: 12 March 2018 / Accepted: 11 August 2018 / Published online: 29 August 2018  
© Springer-Verlag GmbH Germany, part of Springer Nature 2018

## Abstract

An analytical method has been proposed to estimate the leakage from a water-filling tunnel between two reservoirs, based on Darcy's law and the position of the water table, for a phreatic aquifer. The variable water-fill level in the tunnel and an arbitrary intersection angle between the tunnel and horizontal plane were considered. The reliability of this method was validated by numerical analysis and the measured leakage during two water-filling tests in the Heimifeng Pumped Storage Power Station in China. The calculated leakage can represent both the measured value and numerical result due to the small differences between them. Also, the effect of some parameters on the leakage was analysed. Results indicated that leakage increased with decreasing intersection angle, the increase of hydraulic conductivity of the reinforced concrete lining, and the increase of water-fill level in the tunnel. Other parameters exerted little effect on the leakage. Furthermore, the total leakage was estimated under the simultaneous running of two tunnels. When one tunnel was running, the other tunnel was emptying. The calculated leakage was 4.48–8.85 L/s for both tunnels running, which was about 0.5 L/s less than that with one tunnel running and other tunnel emptying. This revealed that the running tunnel had little effect on the leakage from the other (emptying) tunnel.

**Keywords** Analytical solutions · Leakage · Hydraulic pressure tunnel · Sensitivity analysis · Numerical modeling

## Introduction

Long-term leakage from hydraulic/water conveyance tunnels affects the safe operation and economic benefits of a reservoir. These tunnels are often reinforced by a steel lining to resist high internal pressures—examples include Qinglong hydropower station, Jinping-II hydropower station, and Liyang pumped storage power station in China; La Grande-II hydropower station in Canada; Goina hydropower station in India, etc. However, steel linings are complicated and costly to construct and are only used in areas with branch pipes under high internal water pressure in the lower horizontal section in front of some underground powerhouses. The upper horizontal and inclined shaft sections of water conveyance tunnels are

constructed of reinforced concrete; therefore, some leakage is inevitable owing to the partial cracking of the lining under high internal water pressures (Yi et al. 2011; Shin et al. 2012). The estimation of leakage from these tunnels under high internal water pressure during water-filling tests, or normal operation of the reservoir, is deemed necessary.

More research has concentrated on water inflow *into* such tunnels (Hwang and Lu 2007; Zarei et al. 2011; Chiu and Chia 2012; Russo et al. 2013; Chen et al. 2016; Rezae 2017; Su et al. 2017). Many methods, such as analytical solutions and numerical analyses, have been employed to calculate water inflow to conveyance tunnels. Goodman et al. (1965) proposed a steady-state analytical solution to calculate groundwater inflow into a circular tunnel. Based on the Goodman equations, some modified solutions have been presented (Lei 1999; El Tani 2003, 2010; Karlsrud 2001; Moon and Fernandez 2010; Liu et al. 2018). Numerical models of fluid flow into tunnels have also been presented (Molinero et al. 2002; Masset 2011; Farhadian et al. 2016; Nikvar Hassani et al. 2016). Comparisons, in relation to prediction of groundwater inflow into a circular tunnel, between analytical solutions and numerical modeling were conducted by Farhadian et al. (2017) and Nikvar Hassani et al. (2018).

✉ Yong Huang  
hyong@hhu.edu.cn

<sup>1</sup> School of Earth Science and Engineering, Hohai University, 1 Xikang Road, Nanjing 210098, Jiangsu Province, China

<sup>2</sup> Institute of hydrology and water resources, Hohai University, Nanjing 210098, China

The results showed that numerical simulation was more reliable in complex geomechanical and hydrogeological conditions. Some geological factors involved in and/or prior to tunnel construction—fracture or fault zones, fracture aperture width and length, the depth of cover above the tunnel, and the permeability of fractured rocks—have been considered to estimate water inflows (Kitterød et al. 2000; Kværner and Snilsberg 2011; Nilsen and Palmström 2001; Huang et al. 2013; Sharifzadeh et al. 2013; Holmøy and Nilsen 2014; Farhadian et al. 2017).

For a completed tunnel, with its lining, the leakage is mainly related to the permeability of the reinforced concrete lining, the surrounding rock, grouted zones, and fault zones across the tunnel. The groundwater inflow into the tunnel can decrease by 90–95% when using tunnel grouting (Zhang et al. 2015); furthermore, the permeability of the lining and grouting zones will increase with rising water pressure in the tunnel, in particular in the presence of cracks in the lining (Yi et al. 2011).

However, little attention has been paid to the research of leakage from hydraulic pressure tunnels. For unlined water tunnels, the leakage has been estimated by Panthi and Nilsen (2010) and found to be mainly affected by the hydrostatic head and the geometric characteristics of the rocks—such as joint connectivity rate, joint roughness, and joint orientation (Lyu et al. 2018). However, the method could not be applied to lined water tunnels subjected to high internal water pressure because the joints therein were grouted; thus, the leakage only occurs through cracks formed in the concrete lining (Ren et al. 2009). A reinforced concrete lining's design is often based on the assumption that the water pressure acts on the inner surface of the concrete lining. Leakage through the lining will increase with increasing water pressure due to a possible gap between the lining and the grouting zone (Fernandez and Alvarez Jr. 1994; Bobet and Nam 2007). Additionally, with the increase in internal pressure, the width of the cracks in the lining, and the permeability thereof, may be changed due to deformation of the surrounding rocks (Schleiss 1997); therefore, leakage from the tunnel depends on the width of the cracks (Yi et al. 2011). Some coupling processes based on elastic damage theory and groundwater flow theory have been developed (Schleiss 1997; Rong et al. 2006; Bian and Xiao 2010; Shin et al. 2012; Hu et al. 2013). These studies were mainly focused on the analysis of cracks in tunnel linings, and the design of, and loads acting on, the lining. The calculation of leakage was rarely discussed because it was difficult to determine the position, distribution, and number of cracks. In this study, the tunnel, with its reinforced concrete lining, was treated as a homogeneous weak permeable medium without considering the development of cracks in its lining.

The aim of this research was to deduce an analytical solution with which to estimate leakage from a hydraulic pressure tunnel by considering the effects of tunnel length, the

intersection angle between the tunnel and the horizontal plane, the permeability of the lining, and the water filling level. The leakage calculated by using the analytical method was validated using observation data, and sensitivity analysis of the parameters is discussed. The leakage was estimated with the verified analytical method during normal operation of the reservoir, which can provide some basis for subsequent leakage control measurements in hydraulic pressure tunnels.

The work involved analysis of the leakage from a tunnel. Firstly, the location, scale, and configuration of the tunnel, as well as the permeability of the rock surrounding it, were determined; secondly, an analytical solution was developed considering the tunnel as being completely, and partially, filled with water. Finally, the analytical solution was verified and used to assess the amount of leakage from the water-conveyance tunnels in a case study based on Heimifeng Pumped Storage Power Station (HPSPS) in China.

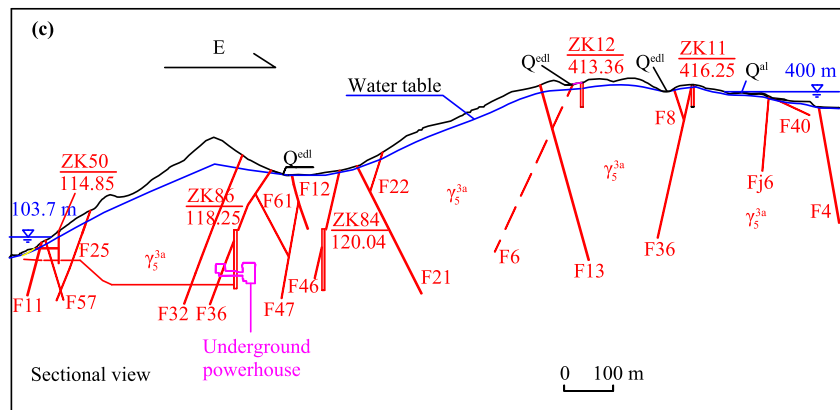
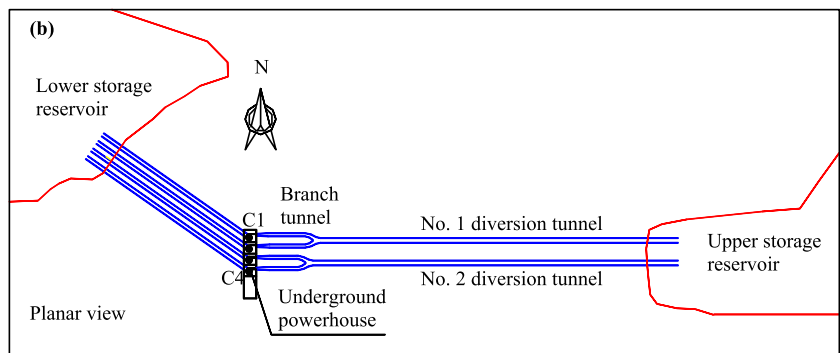
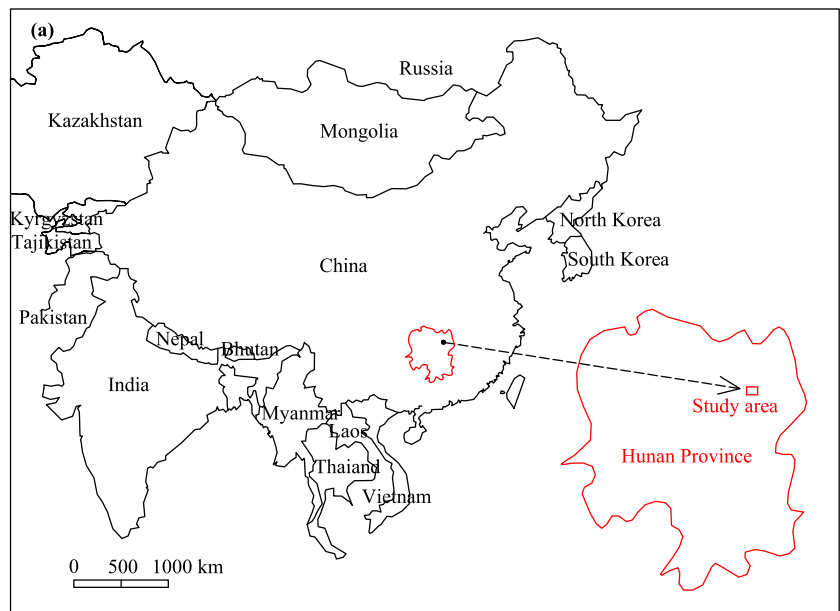
## Research area

### Study site

HPSPS is situated in Wangcheng County, Hunan Province, around 25 km from Changsha City, China. It includes four reversible pumped storage units, and each unit has an installed capacity of 300 MW. It is composed of upper and lower storage reservoirs, an underground powerhouse, and two water-conveyance tunnels (Fig. 1). Water levels above sea level (a.s.l.) for the upper and lower storage reservoirs are 400 and 103.7 m, respectively. The nominal productive head, the minimum water head required for the rated output of a hydraulic turbine under normal operation, is 295 m. The underground powerhouse is located at the tail of the water-conveyance tunnels and close to the lower storage reservoir.

The two water-conveyance tunnels are arranged in parallel at a separation of 46 m and each tunnel has a radius of 4.25 m. Each tunnel corresponds to two pumped storage units, and each unit has two functions: power generation and pumping. Each of the water-conveyance tunnels consists of an upper horizontal section, an inclined shaft section, and a lower horizontal section (Fig. 2a), whereby the upper horizontal section was drilled over a length of 280 m at a slope of 8% from an elevation of 365.5 to 343.25 m a.s.l., while the inclined shaft section was drilled over a length of approximately 420 m at a slope of 50° from an elevation of 341.51 to 17.85 m a.s.l. The lower horizontal section consists of a horizontal segment, a Y-type branch tunnel, and two tailrace tunnels. The lengths of the horizontal segments of the two diversion tunnels (Nos. 1 and 2) are 193.93 and 208.93 m, respectively. A Y-type branch tunnel was arranged to connect the horizontal segment and the corresponding tailrace tunnels for each diversion tunnel (Fig. 2b). Both of the Y-type branch tunnels have a bifurcation

**Fig. 1** **a** Location of Heimifeng Pumped Storage Power Station (HPSPS), China. **b** Layout of the hydraulic structures and **c** geological cross-section

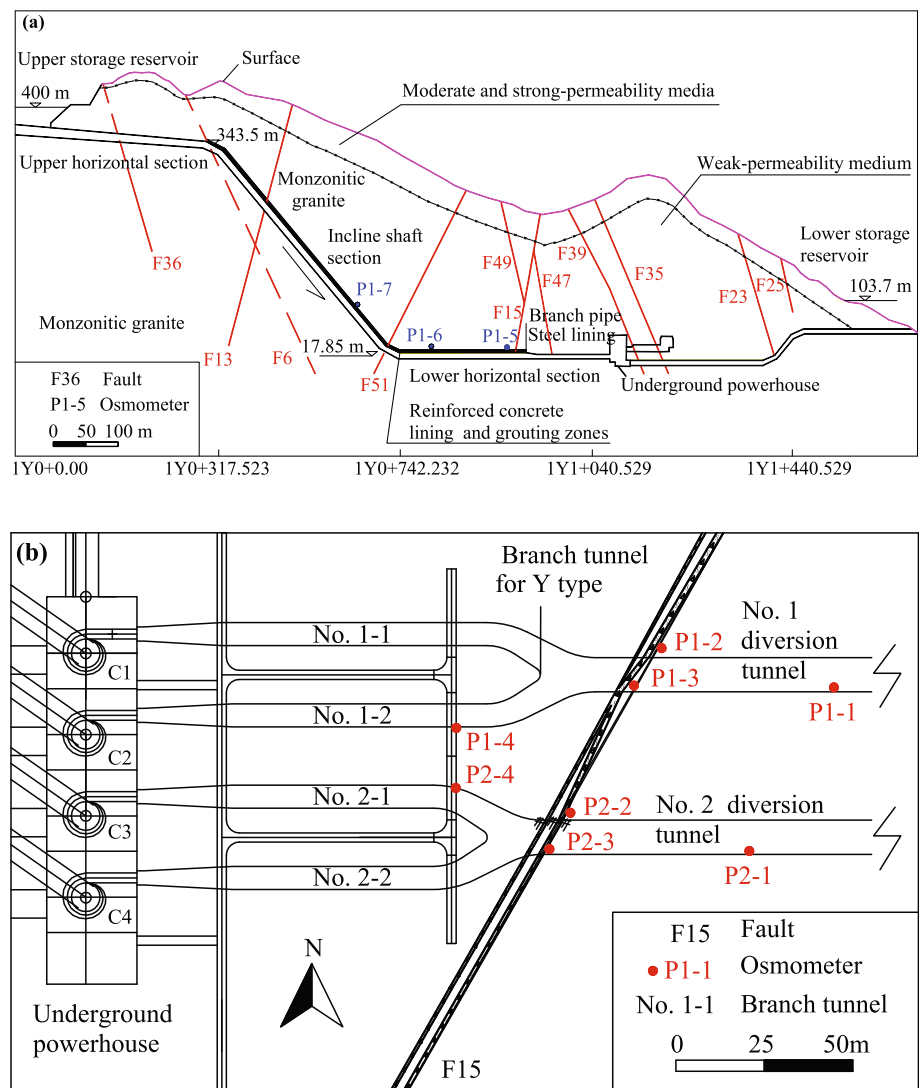


Legend	$Q^{edl}$ Eluvial layer	$\gamma_s^{3a}$ Monzonitic granite	ZK84 Number of borehole
	F Fault	Water table	120.04 Elevation of borehole

angle of  $60^\circ$  and are 24.31 m long and were designed with variable radii from 4.25 m (main tunnel) to 2.65 m (branch tunnel). These branch tunnels were reinforced by using steel plate lining with very low permeability, so that the branch

tunnels are deemed almost impermeable. The two diversion tunnels were strengthened using a reinforced concrete lining with a thickness of 0.5–0.8 m. The chainages covered by the reinforced concrete lining range from 1Y0 + 118.354 to

**Fig. 2** Location of water-conveyance tunnels: **a** No. 1 diversion tunnel, and **b** Branch tunnel



1Y0 + 933.552, where ‘1Y’ refers to the No. 1 diversion tunnel, ‘0’ denotes the centre of the upper storage reservoir, and ‘118.354’ represents the distance to the centre (Fig. 2a) and from 2Y0 + 118.354 to 2Y0 + 948.552 for the diversion tunnels Nos.1 and 2, respectively.

### Geological framework

The area is situated in an area containing low mountains, of which the elevations of the ground surface in the east are generally about 300 m greater than those in the west. Granite in the late Yanshan and Quaternary strata (Q) are revealed across the study site. As shown in Fig. 1a, Monzonitic granite is widely distributed around the water-conveyance tunnels and underground powerhouse. The Quaternary strata such as the eluvial layer ( $Q^{cdl}$ ), riverbed alluvium ( $Q^{al}$ ), and colluvial deposit ( $Q^{col+dl}$ ), are mainly distributed near the ground surface with thicknesses ranging from 2 to 5 m.

The faults revealed in the upper storage reservoir strike N50–70°E and incline NW with a dip angle of 54–78°, whereas the faults shown in the lower storage reservoir strike N43–65°W and incline NE with a dip angle of 55–82°. Additionally, some granitic pegmatite veins lie close to the lower horizontal section with a strike of NE and a width of 0.2 m. Many fractures with steep dip angles of 65° have developed in the area of the underground powerhouse and some of these fractures are filled by granitic pegmatite and quartz veins. Cross-cutting of fractures and faults constitutes the groundwater storage space and conducting pathways. Groundwater is recharged by precipitation and discharged to the gully in the form of spring water through a fractured aquifer system.

### Types and permeability of surrounding rock

According to data from exploratory adits, boreholes, and geophysical tests, the rocks surrounding the tunnels are divided into five types based on the Standard for Engineering

**Table 1** Percentage by type of rocks surrounding the two water-conveyance tunnels

Type of surrounding rocks	No. 1 diversion tunnel			No. 2 diversion tunnel		
	Upper horizontal section	Inclined shaft section	Lower horizontal section	Upper horizontal section	Inclined shaft section	Lower horizontal section
II	100	55	60	32	61	42
III	0	40	18	34	35	42
IV	0	5	22	34	4	16

Classification of Rock Masses (GB50218-94). Integrity and strength indices of rocks become weaker from classes I–V; however, the permeability of the rocks gradually increases from classes I–V. The types of surrounding rocks around two water-conveyance tunnels in HSPS are displayed in Table 1: the rocks surrounding the No. 1 diversion tunnel exhibit better integrity than those around the No. 2 diversion tunnel. The horizontal segments for the two diversion tunnels are about 215 m below ground surface and a fault, F15, is close to two branch tunnels of the ‘Y’-type tunnel. The distance from F15 to the intersection of the main and branch tunnels is 14 m for the No. 1 diversion tunnel and 4 m for the No. 2 diversion tunnel (Fig. 2b); hence, the percentage of rock class IV is larger in the lower horizontal sections due to the effect of F15.

According to results from high water-pressure tests and pumping tests in the field and penetration tests conducted on rock blocks in the laboratory, hydraulic conductivity can be calculated for the different surrounding rocks (Xu et al. 2012; Ma et al. 2014; Wu et al. 2015a, b, 2016, 2017). Hydraulic conductivities of surrounding rocks for types II–IV are  $i \times 10^{-6}$  cm/s,  $i \times 10^{-4}$  to  $i \times 10^{-6}$  cm/s, and  $i \times 10^{-4}$  cm/s, respectively, under natural conditions, where  $i$  is an arbitrary constant between 1 and 10; however, cement and chemical grouts have been used in different types of surrounding rocks. The permeability is increased by between two and four orders of magnitude relative to that prevailing before grouting.

## Methods

### Analytical solution of tunnel leakage

During the normal operation of the reservoir, groundwater in the rock, originating from leakage from the water-conveyance tunnels, has a gradually varying flow rate owing to the changes in the upper and lower reservoir water levels. Eventually, a steady-state flow regime is established. The leakage was governed by the boundary conditions imposed by the reservoirs. Because the minimum thickness of the unsaturated zone is about 60 m, the travel time of

groundwater from the top of the unsaturated zone to the groundwater level is long due to the low permeability of the surrounding rock. The change in groundwater level caused by precipitation is less than that caused by leakage; therefore, it is assumed that (1) rainfall recharge does not need to be considered for this aquifer, (2) the rocks surrounding the tunnels are homogeneous isotropic media, (3) the bottom of the aquifer is horizontal, (4) the groundwater is a gradually varying flow and satisfies Darcy’s law, and (5) water flow along the water-conveyance tunnels from the upper to lower storage reservoirs can be regarded as one-dimensional (1D) owing to the small hydraulic gradient between the two reservoirs. Based on these assumptions, the upper reservoir can be regarded as the left river, and the lower storage reservoir as the right river. The formula for steady flow under a phreatic aquifer between two reservoirs can be expressed as (Bear 1972):

$$h^2 = h_u^2 + \frac{h_l^2 - h_u^2}{l}x \quad (1)$$

where  $h_u$  and  $h_l$  refer to the upper and lower storage reservoir water levels respectively,  $h$  is the phreatic water level at an arbitrary position between the upper and lower storage reservoirs,  $l$  is the horizontal distance between two reservoirs, and  $x$  denotes the position or horizontal coordinate (Fig. 3a).

According to Darcy’s law, leakage or discharge per unit width from water-conveyance tunnels under water filling condition can be given by:

$$q_1 = K_1 \cdot \frac{h_u - h_c}{d_1} \cdot 2\pi R \quad (2)$$

$$q_2 = K_2 \cdot \frac{h_c - h}{d_2} \cdot 2\pi(R + d_1) \quad (3)$$

where  $q_1$  and  $q_2$  represent the leakage per unit width with a concrete lining and the grouting zone in the surrounding rock,  $K_1$  and  $K_2$  denote the hydraulic conductivities of the two grouting zones,  $d_1$  and  $d_2$  represent the thicknesses of the two grouting zones respectively,  $h_c$  is the water-table head above the concrete

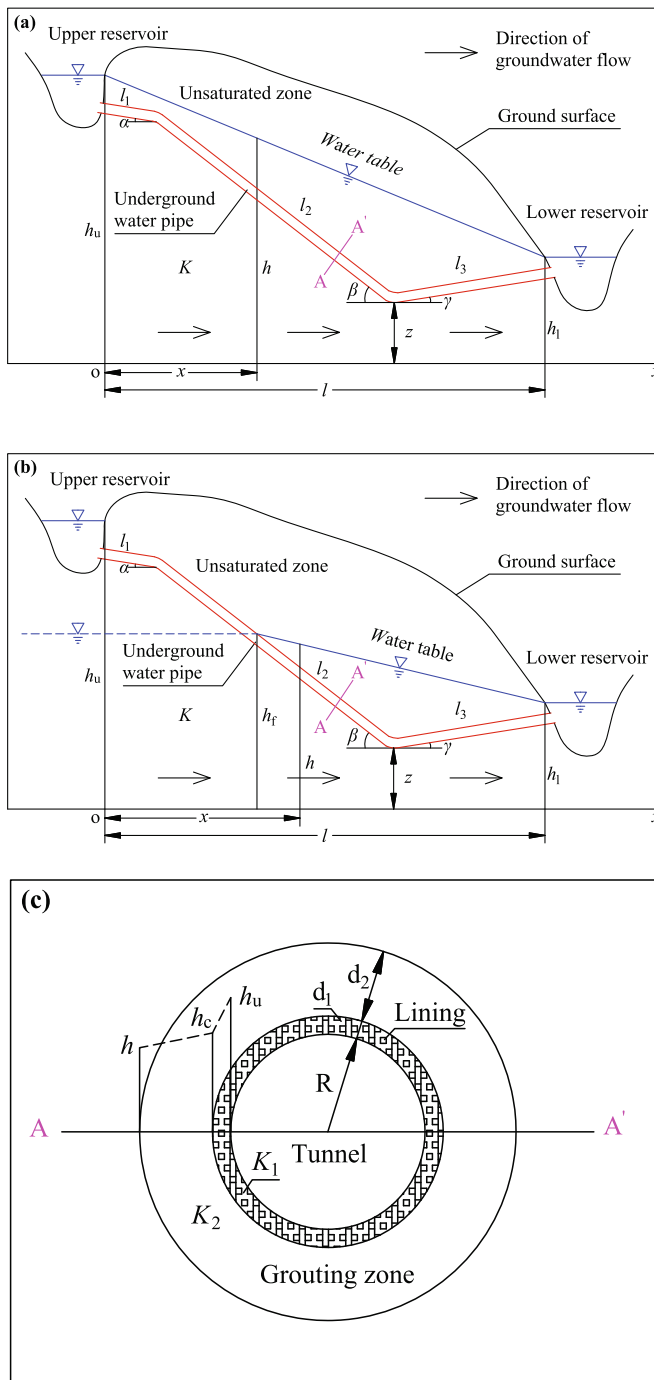


**Fig. 3** Conceptual models for an underground water pipe. **a** Underground water pipe filled with water, **b** underground water pipe part-filled with water, and **c** schematic diagram of tunnel section

lining, and  $R$  is the radius of the water-conveyance tunnel (Fig. 3c). The leakage in any section should be equal under steady flow conditions, and  $q_1 = q_2$ ; hence, using Eqs. (2) and (3),  $h_c$  can be calculated as:

$$h_c = \frac{\pi R d_2 K_1 h_u + \pi (R + d_1) d_1 K_2 h}{\pi (R + d_1) d_1 K_2 + \pi R d_2 K_1} \tag{4}$$

The leakage,  $q$ , can be rewritten as:

$$q = K_1 \cdot \frac{h_u - h}{d'} \cdot 2\pi R \tag{5}$$

$$d' = \frac{(R + d_1) d_1 K_2 + R d_2 K_1}{(R + d_1) K_2} \tag{6}$$

where  $d'$  is defined as an effective hydraulic path. If  $K_1 = K_2 = K$ ,  $d'$  can be rewritten as:

$$d' = d_1 + \frac{R}{R + d_1} \cdot d_2 \tag{7}$$

For a hydraulic conveyance tunnel, the ratio of  $R/d_1$  is often close to, or greater than, 10, so  $d' = d_1 + d_2$ , and the leakage can be expressed as:

$$q = K \cdot \frac{h_u - h}{d_1 + d_2} \cdot 2\pi R \tag{8}$$

Substituting  $h$  from Eq. (1) into Eq. (5), the leakage from a water-conveyance tunnel can be given by:

$$q = K_1 \cdot \left( h_u - \sqrt{h_u^2 + \frac{h_1^2 - h_u^2}{l} x} \right) \cdot \frac{2\pi R}{d'} \tag{9}$$

Thus, for filled (1) and part-filled (2) tunnels:

1. When a water-conveyance tunnel is filled with water, the total leakage from the tunnel is the sum of the leakages from the upper horizontal section, inclined shaft section, and lower horizontal section (Fig. 3a). Therefore, the total leakage,  $Q$ , can be expressed as:

$$Q = Q_1 + Q_2 + Q_3 = \int_0^{l_1 \cos \alpha} q dx + \int_{l_1 \cos \alpha}^{l_1 \cos \alpha + l_2 \cos \beta} q dx + \int_{l_1 \cos \alpha + l_2 \cos \beta}^{l_1 \cos \alpha + l_2 \cos \beta + l_3 \cos \gamma} q dx \tag{10}$$

where  $Q_1$ ,  $Q_2$ , and  $Q_3$  denote the leakages from the upper horizontal, inclined shaft, and lower horizontal sections  $l_1$ ,  $l_2$ , and  $l_3$  respectively.  $\alpha$ ,  $\beta$ , and  $\gamma$  are the intersection angles between the horizontal plane and each of the three sections, respectively.

Substituting Eq. (9) into Eq. (10),  $Q_1$ ,  $Q_2$ , and  $Q_3$  can be rewritten as:

$$Q_1 = \int_0^{l_1 \cos \alpha} K_1 \cdot \left( h_u - \sqrt{h_u^2 + \frac{h_1^2 - h_u^2}{l} x} \right) \cdot \frac{2\pi R}{d'} dx = K_1 \cdot \frac{2\pi R}{d'} \cdot \left[ h_u l_1 \cos \alpha - \frac{2}{3} \cdot \frac{l}{h_1^2 - h_u^2} \cdot (H_1^3 - h_u^3) \right] \tag{11}$$

$$Q_2 = \int_{l_1 \cos \alpha}^{l_1 \cos \alpha + l_2 \cos \beta} K_1 \cdot \left( h_u - \sqrt{h_u^2 + \frac{h_1^2 - h_u^2}{l} x} \right) \cdot \frac{2\pi R}{d'} dx \tag{12}$$

$$= K_1 \cdot \frac{2\pi R}{d'} \cdot \left[ h_u l_2 \cos \beta - \frac{2}{3} \cdot \frac{l}{h_1^2 - h_u^2} \cdot (H_2^3 - H_1^3) \right]$$

$$Q_3 = \int_{l_1 \cos \alpha + l_2 \cos \beta}^{l_1 \cos \alpha + l_2 \cos \beta + l_3 \cos \gamma} K_1 \cdot \left( h_u - \sqrt{h_u^2 + \frac{h_1^2 - h_u^2}{l} x} \right) \cdot \frac{2\pi R}{d'} dx \tag{13}$$

$$= K_1 \cdot \frac{2\pi R}{d'} \cdot \left[ h_u l_3 \cos \gamma - \frac{2}{3} \cdot \frac{l}{h_1^2 - h_u^2} \cdot (H_3^3 - H_2^3) \right]$$

where

$$H_1 = \sqrt{h_u^2 + \frac{h_1^2 - h_u^2}{l} \cdot l_1 \cos \alpha} \tag{14}$$

$$H_2 = \sqrt{h_u^2 + \frac{h_1^2 - h_u^2}{l} \cdot (l_1 \cos \alpha + l_2 \cos \beta)} \tag{15}$$

$$H_3 = \sqrt{h_u^2 + \frac{h_1^2 - h_u^2}{l} \cdot (l_1 \cos \alpha + l_2 \cos \beta + l_3 \cos \gamma)} \tag{16}$$

2. When a water-conveyance tunnel is part-filled with reservoir water (Fig. 3b), if  $0 < x \leq l_1 \cos \alpha$ ,  $Q_1$ ,  $Q_2$ , and  $Q_3$  can be rewritten as:

$$Q_1 = \int_{l_1 \cos \alpha - (h_f - l_2 \sin \beta - z) / \tan \alpha}^{l_1 \cos \alpha} K_1 \cdot \left( h_f - \sqrt{h_f^2 + \frac{h_1^2 - h_f^2}{l} x} \right) \cdot \frac{2\pi R}{d'} dx \tag{17}$$

$$= K_1 \cdot \frac{2\pi R}{d'} \cdot \left[ h_f (h_f - l_2 \sin \beta - z) / \tan \alpha - \frac{2}{3} \cdot \frac{l}{h_1^2 - h_f^2} \cdot (I_1^3 - I_0^3) \right]$$

$$Q_2 = \int_{l_1 \cos \alpha}^{l_1 \cos \alpha + l_2 \cos \beta} K_1 \cdot \left( h_f - \sqrt{h_f^2 + \frac{h_1^2 - h_f^2}{l} x} \right) \cdot \frac{2\pi R}{d'} dx \tag{18}$$

$$= K_1 \cdot \frac{2\pi R}{d'} \cdot \left[ h_f l_2 \cos \beta - \frac{2}{3} \cdot \frac{l}{h_1^2 - h_f^2} \cdot (I_2^3 - I_1^3) \right]$$

$$Q_3 = \int_{l_1 \cos \alpha + l_2 \cos \beta}^{l_1 \cos \alpha + l_2 \cos \beta + l_3 \cos \gamma} K_1 \cdot \left( h_f - \sqrt{h_f^2 + \frac{h_1^2 - h_f^2}{l} x} \right) \cdot \frac{2\pi R}{d'} dx \tag{19}$$

$$= K_1 \cdot \frac{2\pi R}{d'} \cdot \left[ h_f l_3 \cos \gamma - \frac{2}{3} \cdot \frac{l}{h_1^2 - h_f^2} \cdot (I_3^3 - I_2^3) \right]$$

where

$$l' = (h_f - l_2 \sin \beta - z) / \tan \alpha + l_2 \cos \beta + l_3 \cos \gamma \tag{20}$$

$$I_0 = \sqrt{h_f^2 + \frac{h_1^2 - h_f^2}{l'} \cdot [l_1 \cos \alpha - (h_f - l_2 \sin \beta - z) / \tan \alpha]} \tag{21}$$

$$I_1 = \sqrt{h_f^2 + \frac{h_1^2 - h_f^2}{l'} \cdot l_1 \cos \alpha} \tag{22}$$

$$I_2 = \sqrt{h_f^2 + \frac{h_1^2 - h_f^2}{l'} \cdot (l_1 \cos \alpha + l_2 \cos \beta)} \tag{23}$$

$$I_3 = \sqrt{h_f^2 + \frac{h_1^2 - h_f^2}{l'} \cdot (l_1 \cos \alpha + l_2 \cos \beta + l_3 \cos \gamma)} \tag{24}$$

If  $l_1 \cos \alpha < x \leq l_1 \cos \alpha + l_2 \cos \beta$ ,  $Q_1 = 0$ , and  $Q_2$  and  $Q_3$  can be rewritten as:

$$Q_2 = \int_{l_1 \cos \alpha + l_2 \cos \beta - (h_f - z) / \tan \beta}^{l_1 \cos \alpha + l_2 \cos \beta} K_1 \cdot \left( h_f - \sqrt{h_f^2 + \frac{h_1^2 - h_f^2}{l''} x} \right) \cdot \frac{2\pi R}{d'} dx \tag{25}$$

$$= K_1 \cdot \frac{2\pi R}{d'} \cdot \left[ h_f (h_f - z) / \tan \beta - \frac{2}{3} \cdot \frac{l''}{h_1^2 - h_f^2} \cdot (J_2^3 - J_1^3) \right]$$

$$Q_3 = \int_{l_1 \cos \alpha + l_2 \cos \beta}^{l_1 \cos \alpha + l_2 \cos \beta + l_3 \cos \gamma} K_1 \cdot \left( h_f - \sqrt{h_f^2 + \frac{h_1^2 - h_f^2}{l''} x} \right) \cdot \frac{2\pi R}{d'} dx \tag{26}$$

$$= K_1 \cdot \frac{2\pi R}{d'} \cdot \left[ h_f l_3 \cos \gamma - \frac{2}{3} \cdot \frac{l''}{h_1^2 - h_f^2} \cdot (J_3^3 - J_2^3) \right]$$

where

$$l'' = (h_f - z) / \tan \beta + l_3 \cos \gamma \tag{27}$$

$$J_1 = \sqrt{h_f^2 + \frac{h_1^2 - h_f^2}{l''} \cdot [l_1 \cos \alpha + l_2 \cos \beta - (h_f - z) / \tan \beta]} \tag{28}$$

$$J_2 = \sqrt{h_f^2 + \frac{h_1^2 - h_f^2}{l''} \cdot (l_1 \cos \alpha + l_2 \cos \beta)} \tag{29}$$

$$J_3 = \sqrt{h_f^2 + \frac{h_1^2 - h_f^2}{l''} \cdot (l_1 \cos \alpha + l_2 \cos \beta + l_3 \cos \gamma)} \tag{30}$$

where  $h_f$  is the water level in the tunnel, and  $z$  is the distance between the bottom of the inclined shaft section and the bottom of the aquifer. The water level in the tunnel,  $h_f$ , changed over time during impoundment, and  $h_u$  and  $h_1$  will also change during the operation of the reservoir, so the water levels are therefore a function of time. This proposed formula can also be applied to transient flow.

## Leakage calculation under a variable filling level

The water-filling level with an effect on total leakage,  $Q$ , is an instantaneous water level at time  $t$ . If the change in filling level is a piecewise function, the total leakage can be given by:

$$Q = \sum_{i=1}^n \int_{t_i}^{t_{i+1}} Q_i dt \quad (31)$$

where  $Q_i$  is the leakage at  $t$ ,  $i$  is a time period number, and  $n$  is the total number of time periods.

## Numerical solution

In addition to analytical solutions, the leakage from the tunnels was also calculated by using FEFLOW (Finite Element Subsurface FLOW and Transport Simulation System) software, which was developed by DHI-WASY GmbH, Institute for Water Resources Planning and Systems Research Ltd. It is a three-dimensional (3D) variably saturated subsurface flow and solute transport model that can describe the spatial and temporal distribution of groundwater. FEFLOW has been universally applied to the simulation of groundwater flow in porous and fractured media (Sefelnasr et al. 2014; Hu and Jiao 2015; Malott et al. 2016; Kavour et al. 2017). To compare this with the analytical solution, a 2D numerical model based on FEFLOW was employed to calculate the leakage. The left and right-hand sides of the model have the first-type (Dirichlet) boundary, which corresponds to the upper and lower reservoir water levels, respectively. The bottom of model has the second-type (Neumann) boundary. It has weak permeability and is considered to be an aquiclude. The top of the model is a free surface boundary. The hydraulic pressure tunnels form the first-type boundary.

## Method of error estimation

The difference between the measured and calculated leakages was estimated by use of root mean squared error (RMSE) measurement. This is the mean average of the squared differences between measured and calculated leakages. Thus,

$$\text{RMSE} = \left[ \frac{1}{n} \sum_{i=1}^n (Q_m - Q_c)_i^2 \right]^{1/2} \quad (32)$$

where  $n$  is the number of time steps, and  $Q_m$  and  $Q_c$  are the measured and calculated leakages, respectively.

## Results and discussion

### Water-filling tests

Two groups of water-filling tests have been conducted to verify the reliability of the water-conveyance tunnels. The test of the No. 1 diversion tunnel ran from 4 April 2009 to 14 May 2009. Water levels in the lower and upper storage reservoirs remained at 87.26 and 381.5 m, respectively, upon test completion. The test of the No. 2 diversion tunnel ran from 16 to 30 November 2009. At this time, water levels in the lower and upper storage reservoir remained at 78.61 and 388.25 m, respectively. Test records are listed in Table 2. The time between the two tests is about half a year; thus, the design condition means that No. 1 diversion tunnel was filled with water and No. 2 diversion tunnel was emptied. The water levels and fluxes could be observed in the No. 2 diversion tunnel. When the No. 2 diversion tunnel was filled with water, the normal operation of the HPSPS could be simulated.

### Osmometer data

An osmometer is a sensor for measuring pore water pressure in structures. The purpose of using an osmometer is to estimate the leakage in the tunnels. Osmometers P1-1 to P1-4 are located at chainage 1Y0 + 912, F15, and No. 1-2 branch tunnel for monitoring the No. 1 diversion tunnel (Fig. 2b). At F15, the elevations of P1-2 and P1-3 are 22 and 36.94 m, respectively; however, P2-1, P2-2, P2-3, and P2-4 are located at chainage 2Y0 + 948.5, F15, and No. 2-1 branch tunnel for the No. 2 diversion tunnel (Fig. 2b). The elevations of P2-2 and P2-3 are 22 and 35.44 m. Measured data from the eight osmometers are illustrated in Fig. 4. The water table at P1-1 is at about 96 m a.s.l. with an increase of 75 m after the water-filling test of the No. 1 diversion tunnel (the first test). The water table remained stable even during the second test period, which means that the water-filling test of No. 2 diversion tunnel (the second test) has not affected the water table at P1-1. Measured data from P1-2 increase over the two tests, but the extent of the increase in the second test is smaller than that of the first test. The water table at P1-3 rises after the first test by more than 300 m, which indicates leakage under the high water pressure; however, P1-3 is unaffected by the second test. For P1-4, there are two peak values of groundwater level during testing, but the increase during the first test exceeds that in the second test. Water tables at P2-1, P2-2, and P2-4 increase after the second test, but the first test has no distinct effect thereon and the first test has little effect on P2-3, whereby the water table increases by about 280 m, and the increase during the second test exceeds that in the first test. The preceding analysis shows that the tunnels will leak during water filling and that the leakages are mainly distributed



**Table 2** Test records: Nos. 1 and 2 diversion tunnels

Diversion tunnel	Location	Change of filling water level (m)	Times of filling water (h)	Rising velocity of water level (m/h)	Steady time of water level (h)
No. 1	Lower horizontal section	2.7–22.1	11.467	1.692	13.53
	Inclined shaft section	22.1–82.0	6.667	8.985	9.17
		82.0–140.0	10.133	5.724	23.95
		140.0–220.0	11.333	7.059	50.0
		220.0–280.0	9.0	6.667	48.82
		280.0–338.4	12.767	0.457	48.15
	Upper horizontal section	338.4–381.5	4.0	10.77	72.0
No. 2	Lower horizontal section	13.6–19.6	8.383	0.716	9.6
	Inclined shaft section	19.6–141.6	15.733	7.754	24.15
		141.6–220	7.717	10.237	47.8
		220.6–280.6	6.15	9.756	48.0
	Upper horizontal section	280.6–341.6	11.933	5.111	66.267
	Upper horizontal section	341.6–388.25	13.4	3.481	72.0

around the tunnels; thus, the leakage can be calculated using the proposed method.

### Monitoring and calculating leakage around the tunnels

Some measurement points such as drainage ditches, measuring weirs, drainage galleries around the tunnels, and the No. 2 diversion tunnel, were used to monitor leakage during the first test. When the second test was performed, the Nos. 1 and 2 diversion tunnels were filled with water. The main measurement points for leakage determination were drainage ditches, measuring weirs, and drainage galleries. Measured data from the first test show leakage rates ranging from 1.0 to 3.32 L/s with an average value of 2.1 L/s. The

minimum value was measured at 12:00, 3 May 2009, and the maximum value was measured at 6:00, 14 May 2009. Leakage increases with increasing water level (Fig. 5a). The leakage increases from 0.66 to 1.29 L/s with an average value of 0.89 L/s. The measured leakage increases until 28 November 2009, and then decreases and remains stable (Fig. 5b). Comparison between the first and second tests indicates that the leakage from the former is larger than that from the latter. This may be caused by water pressure around the No. 1 diversion tunnel, where the leakage from the No. 1 diversion tunnel increases the external water pressure in the No. 2 diversion tunnel, which reduces leakage at the No. 2 diversion tunnel.

The leakage was calculated by using the proposed analytical formula and its numerical solution. Values of hydraulic conductivity and tunnel parameters are listed in Table 3. The absolute errors and RMSE were used to estimate how well the calculated leakages agree with the observed values. Also, the Nash-Sutcliffe model efficiency coefficient (NSMEC) was used to assess the goodness of fit (Nash and Sutcliffe 1970). The calculated leakage was similar to the changes in water level in the first test, which underestimated the measured leakage (Fig. 5a). The absolute errors range from 0.01 to 0.42 L/s and the RMSE is 0.241 L/s with an NS coefficient of 0.928 (Table 4). In the second test, the calculated leakage exceeds that measured (Fig. 5b) with the absolute errors ranging from 0.01 to 0.18 L/s and the RMSE indicated as 0.11 L/s with an NS coefficient of 0.84 (Table 4). The differences between measured leakages and the numerical results are listed in Table 4. Compared with the analytical solution, the numerical solution differs slightly in terms of

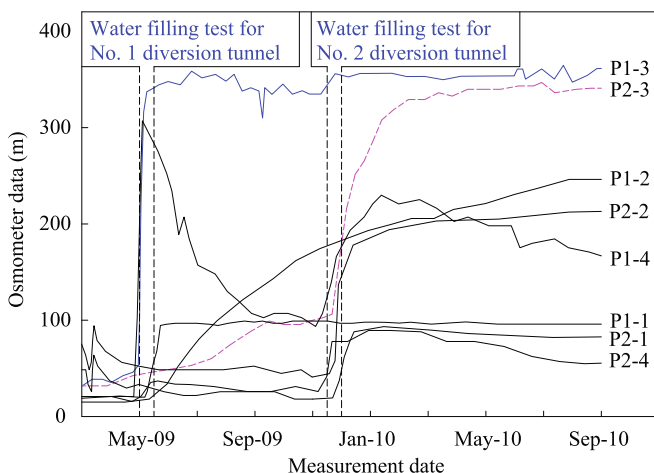
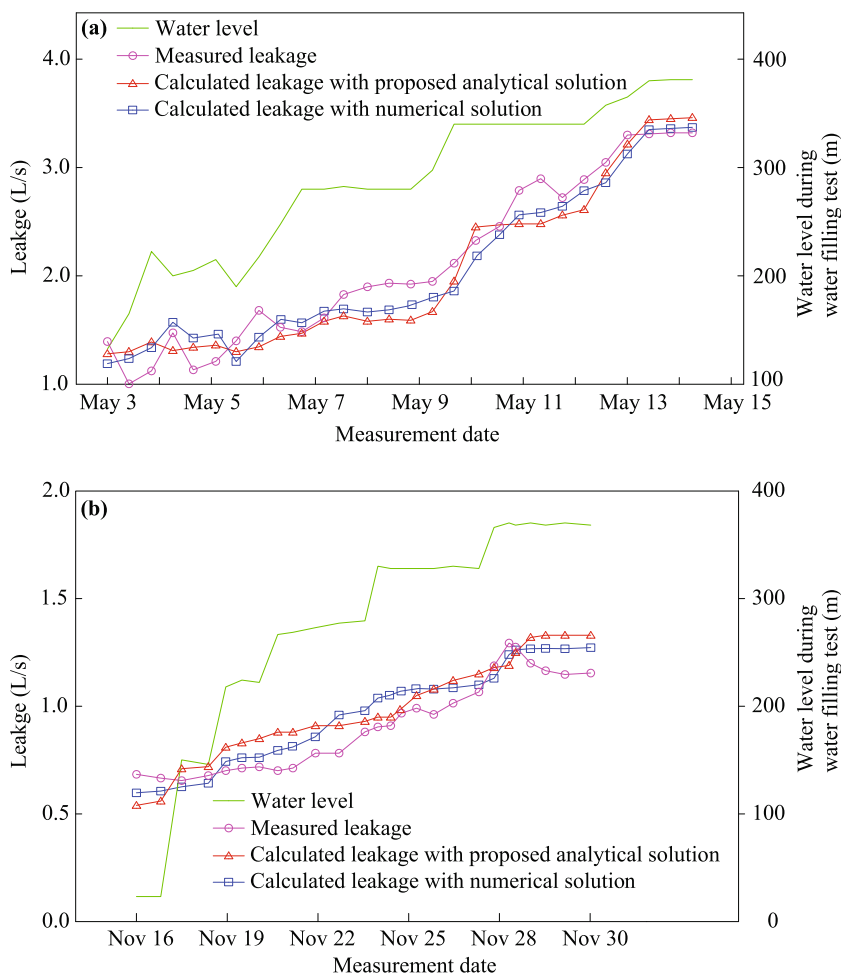


**Fig. 4** Osmometer data versus time: water-filling tests

**Fig. 5** Comparison of calculated and measured leakage for the **a** first test, and **b** second test



the absolute errors, RMSE, and large NSMEC, but the difference between them is negligible as it lies within pre-specified tolerances. The analytical solution can, therefore, be used to estimate the leakage from a tunnel during reservoir operations.

**Sensitivity analysis**

**Effect of  $\beta$  on leakage**

$\beta$  denotes the intersection angle between the inclined shaft section and horizontal plane. For many waterpower projects, it is designed to have differing values. The values are here assumed to lie within the range from 30–80° during sensitivity analysis. When the distance between the upper and lower storage reservoirs ( $l$ ) and  $l_2$  is constant,  $l_1$  will change owing to the different value of  $\beta$ ; therefore,  $l_1/l_2$  is also considered to be a variable, but other parameters in Table 3 remain unchanged. A dimensionless ratio,  $Q/Q_0$ , is used to evaluate the effect of  $\beta$  on leakage, where  $Q_0$  is the leakage at  $\beta = 50^\circ$ . The relationship between  $Q/Q_0$  and  $\beta$  is plotted in Fig. 6: leakage decreases with increasing  $\beta$  when  $l_1/l_2$  is a

constant and the decrease ranges from 0.035 to 0.052 L/s per increment in  $\beta$ . The average decrement in leakage is about 2.8% compared with that at  $\beta = 50^\circ$ ; consequently,  $\beta$  affects

**Table 3** Parameters of calculating the leakage

Parameter	Diversion tunnel	
	No. 1	No. 2
$K_1$ (cm/s)	$1 \times 10^{-7}$	$1 \times 10^{-7}$
$K_2$ (cm/s)	$1 \times 10^{-5}$	$1 \times 10^{-5}$
$d_1$ (m)	0.5	0.5
$d_2$ (m)	5	5
$R$ (m)	4.5	4.5
$h_u$ (m)	400	400
$h_l$ (m)	100	100
$l$ (m)	1,425	1,373
$l_1$ (m)	450	342
$l_2$ (m)	422	422
$\alpha$ (°)	4	5
$\beta$ (°)	50	50
$\gamma$ (°)	0	0

**Table 4** Errors between the measured and calculated leakages

Method	First test			Second test		
	Absolute error	RMSE	NSMEC	Absolute error	RMSE	NSMEC
Comparison with analytical solutions	0.01–0.42	0.241	0.928	0.01–0.18	0.11	0.84
Comparison with numerical solutions	0.02–0.38	0.203	0.941	0.01–0.16	0.084	0.90

the leakage. When  $\beta$  is a constant, leakage decreases with increasing  $l_1/l_2$ , but the decrease diminishes and the average decrement in leakage changes from 2.8 to 0.09% with increasing  $l_1/l_2$ , so the leakage will increase for small  $l_1$  and large  $l_2$ . This may be correct for a single tunnel, but if there are two parallel distributed tunnels, and one tunnel has an effect on the other, and the leakage may change in the opposite direction—for example, the leakage from the second test is smaller than that of the first test although  $l_1$  from the No. 2 diversion tunnel is less than that from the No. 1 diversion tunnel (Table 3).

**Effect of hydraulic conductivity**

During testing and in the operation of the reservoir, the reinforced concrete lining around the tunnel may be cracked under the high water pressure. The hydraulic conductivity of the reinforced concrete lining will increase compared to its design value. Its effect on the leakage is discussed from the perspective of the results of water-filling tests. The ratio of hydraulic conductivity for reinforced concrete lining to that of the grouting zone ( $K_1/K_2$ ) is taken as the independent variable ( $X$ -axis), and  $Q/Q_0$  plotted on the  $Y$ -axis (Fig. 7); the solid triangles denote calculated leakage, and the dotted line is a fitting curve. The  $K_2$  value is  $1 \times 10^{-5}$  cm/s, but  $K_1$  values are  $1 \times 10^{-7}$ ,  $5 \times 10^{-7}$ ,  $1 \times 10^{-6}$ ,  $5 \times 10^{-6}$ , and  $1 \times 10^{-5}$  cm/s, respectively. Figure 7 illustrates that the leakage increases

with increasing  $K_1/K_2$ . The leakage increment is large for small  $K_1/K_2$ ; however, if the  $K_1$  value is doubled, the leakage is increased 2.5-fold. When  $K_1$  is close to  $K_2$ , the leakage increment becomes very small—for example, when the  $K_1$  value is doubled, the leakage is only increased 1.05-fold. The relationship between them is nonlinear. The fitting curve may be described by a single logarithmic relationship:  $Q/Q_0 = 2.25 \ln(K_1/K_2) + 11.03$  with a correlation coefficient of 0.99. Therefore, as predicted, the hydraulic conductivity of the reinforced concrete lining is an important factor affecting the leakage.

Furthermore, the leakage also increases with increasing difference in the water levels between the upper and lower storage reservoirs. The leakage increases with rising water levels in the tunnel. The values of  $\alpha$  and  $\gamma$  are usually smaller than  $5^\circ$ , showing no obvious effect on the leakage.

**Prediction of the leakage with the analytical formula**

After the water-filling tests were completed in 2009, two pumped storage units, Nos. 1-1 and 1-2 from the No. 1 diversion tunnel, have been run since 1 June 2010. The other two pumped storage units, Nos. 2-1 and 2-2 from the No. 2 diversion tunnels, have been run since 6 October 2010. Some measured data from osmometers (numbered P1-1 to P1-4 and P2-1 to P2-4) are shown in Fig. 4. Furthermore, other osmometers were installed in the diversion tunnels between the grouting zone and surrounding rock in August 2008 (Fig. 2a). The osmometer readings are recorded in Table 5) where it can be seen that the water level is decreased by 80 to –130 m when the water in the diversion tunnels leaks into the surrounding rock through the reinforced concrete lining and grouting zone.

Based on the analytical method, the leakage around these two tunnels was estimated during normal operation of the reservoir. For a pumped storage power station, pumping and emptying water are conducted alternately. It is assumed that water from the lower storage reservoir was pumped into the upper storage reservoir from 9:00 pm to 7:00 am the following morning, due to the lower cost of electricity during those hours. The water filling level ranges from the dead storage level (376.5 m) to the normal impounded level (400 m; Fig. 8). Then water from the upper storage reservoir was discharged to generate electricity from 7:00 am to 9:00 pm owing to the high cost of

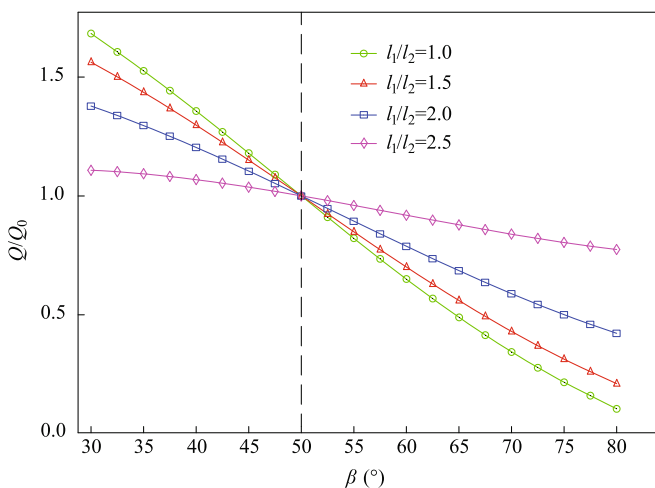
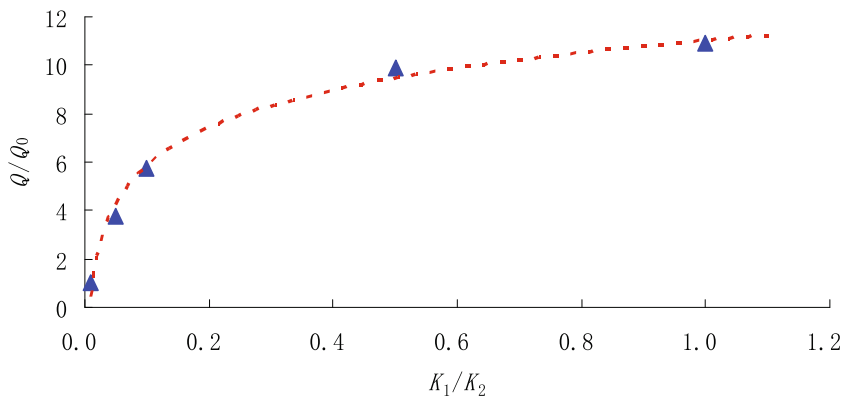


**Fig. 6** Relationship between  $Q/Q_0$  and  $\beta$

**Fig. 7** Relationship between  $Q/Q_0$  and hydraulic conductivity of the reinforced concrete lining



electricity during those hours. The lowest water level is no less than 376.5 m during the generation period. After a period of reservoir operation, one tunnel needs to be examined and repaired, and the other tunnel will keep running. The leakage for this scenario was also calculated (Fig. 8).

The leakage increases during pumping and decreases during emptying (Fig. 8). When the two tunnels are running at the same time, the leakage ranges from 4.48 L/s (387.07 m<sup>3</sup>/day) to 8.85 L/s (764.64 m<sup>3</sup>/day), which is very close to the maximum measured value of 8.0 L/s. When the No. 1 diversion tunnel is filling and No. 2 is emptying, the leakage is between 3.30 L/s to 5.05 L/s, which is more than the leakage when No. 1 is emptying and No. 2 is filling. The total leakage for these two cases is greater than 0.5 L/s for water filling in both tunnels. This leakage is approximately 8.5% of the total leakage and indicates that, when the two tunnels are running simultaneously, one tunnel has little effect on the leakage of the other. The effect indicates a small increase of water pressure and a small decrease in the leakage.

### Conclusions

The analytical formulae for calculating leakage from tunnels with variable water filling levels and an arbitrary angle were deduced, according to Darcy’s law and the formula for steady

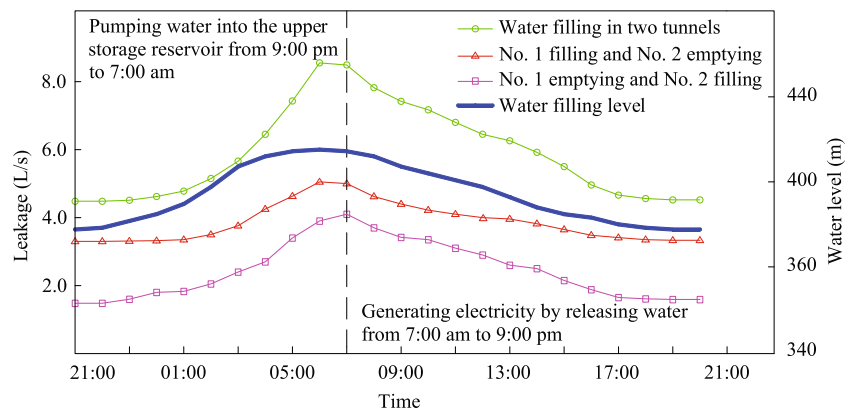
flow under phreatic aquifer conditions, between two reservoirs. The leakage calculated using the analytical method has been validated by the calculated leakage and the measured values from two water-filling tests undertaken at the HSPS site. The small discrepancies indicated that the calculated leakage matched measured values and the proposed method can be used to estimate leakage from the tunnels during reservoir operations. The effects of parameters such as the intersection angle ( $\beta$ ), the hydraulic conductivity of the reinforced concrete lining, and water level, on the leakage have been discussed based on the dimensionless expressions  $Q/Q_0$ ,  $K_1/K_2$ , and  $l_1/l_2$ . The results show that the average decrement in leakage is about 2.8% per increment in  $\beta$ , which implies  $\beta$  does influence the leakage. For different values of the ratio  $K_1/K_2$ , if the  $K_1$  value is doubled, the increase in leakage is 1.05–2.5 times the original leakage. Therefore, the hydraulic conductivity of the reinforced concrete lining is also an important factor influencing the leakage in these cases; furthermore, the leakage increases with rising water level in the tunnels. The effects of other parameters ( $l_1$ ,  $l_2$ ,  $\alpha$ , and  $\gamma$ ) are negligible.

The leakage was estimated during normal reservoir operation by using the proposed analytical method. When both tunnels were running simultaneously, the estimated leakage ranges from 4.48 to 8.85 L/s. If one tunnel is filling and the other tunnel is emptying, the calculated total leakage is more than 0.5 L/s for water filling in both tunnels, which reveals

**Table 5** Observed water level from osmometers during normal operation of the reservoir

Diversion tunnel	Osmometer	Location	Osmometer depth (m)	Maximum water-filling level (m a.s.l.)	New water level in the tunnel (m a.s.l.)	New osmometer reading (m a.s.l.)
No.1	P1-5	1Y0+892	35	388.25	368.5	265.5
	P1-6	1Y0+790	35	388.25	368.5	287.6
	P1-7	1Y0+676	95	388.25	368.5	235.8
No.2	P2-5	2Y0+947	35	392.5	372.5	277.7
	P2-6	2Y0+810	35	392.5	372.5	295.5
	P2-7	2Y0+664	95	392.5	372.5	241.3

**Fig. 8** Estimation of leakage during reservoir operation



that the running tunnel has little effect on the leakage when the other tunnel is emptying. When the reservoir level is 376.5 m, the corresponding reservoir capacity is  $152.6 \times 10^4 \text{ m}^3$ . The estimated total leakage from the reservoir is about  $700 \text{ m}^3$  (0.046% of reservoir capacity by volume), which indicates that the leakage control measures are relatively effective.

**Funding information** This study was financially supported by The National Natural Science Foundation of China (Grant No. 41572209), and sponsored by a Qing Lan Project of Jiangsu Province (2016B16073).

## References

- Bear J (1972) Dynamics of fluids in porous media. Elsevier, Boston, pp 155–286
- Bian K, Xiao M (2010) Research on seepage of high pressure hydraulic tunnel when reinforced concrete lining cracking. *Chin J Rock Mech Eng* 29(2):3647–3654
- Bobet A, Nam SW (2007) Stresses around pressure tunnels with semi-permeable liners. *Rock Mech Rock Eng* 40(3):287–315
- Chen YF, Hong JM, Zheng HK, Li Y, Hu R (2016) Evaluation of groundwater leakage into a drainage tunnel in Jinping-I Arch Dam foundation in Southwestern China: a case study. *Rock Eng* 49(3):961–979
- Chiu YC, Chia Y (2012) The impact of groundwater discharge to the Hsueh-Shan tunnel on the water resources in northern Taiwan. *Hydrogeol J* 20(8):1599–1611
- El Tani M (2003) Circular tunnel in a semi-infinite aquifer. *Tunnel Underground Space Technol* 18:49–55
- El Tani M (2010) Helmholtz evolution of a semi-infinite aquifer drained by a circular tunnel. *Tunnel Underground Space Technol* 25:54–62
- Farhadian H, Katibeh H, Huggenberger P (2016) Empirical model for estimating groundwater flow into tunnel in discontinuous rock masses. *Environ Earth Sci* 75(6):1–16
- Farhadian H, Hassani AN, Katibeh H (2017) Groundwater inflow assessment to Karaj water conveyance tunnel, northern Iran. *KSCE J Civ Eng* 21(6):2429–2438
- Fernandez G, Alvarez TA Jr (1994) Seepage-induced effective stresses and water pressures around pressure tunnels. *J Geotech Eng ASCE* 120(1):108–128
- Goodman R, Moye D, Schalkwyk A, Javendel I (1965) Groundwater inflow during tunnel driving. *Eng Geol* 1:150–162
- Holmøy KH, Nilsen B (2014) Significance of geological parameters for predicting water inflow in hard rock tunnels. *Rock Mech Rock Eng* 47:853–868
- Hu LT, Jiao JJ (2015) Calibration of a large-scale groundwater flow model using GRACE data: a case study in the Qaidam Basin, China. *Hydrogeol J* 23(7):1305–1317
- Hu YJ, Fang JP, Huang DJ, Feng SN, Su XT (2013) Coupling analysis of seepage-stress-cracking for inner water exosmosis of pressure tunnel (in Chinese). *J Beijing Univ Technol* 39(2):174–179
- Huang Y, Yu ZB, Zhou ZF (2013) Simulating groundwater inflow in the underground tunnel with a coupled fracture-matrix model. *J Hydrol Eng* 18(11):1557–1561
- Hwang JH, Lu CC (2007) A semi-analytical method for analyzing the tunnel water inflow. *Tunnel Underground Space Technol* 22(1):39–46
- Karlsrud K (2001) Water control when tunneling under urban areas in the Oslo region. NFF publication No. 12, NFF, Brisbane, Australia, pp 4–33
- Kavour KP, Karatzas GP, Plagnes V (2017) A coupled groundwater-flow-modelling and vulnerability-mapping methodology for karstic terrain management. *Hydrogeol J* 25(5):1301–1317
- Kitterød NO, Colleuille H, Wong WK, Pedersen TS (2000) Simulation of groundwater drainage into a tunnel in fractured rock and numerical analysis of leakage remediation, Romeriksporten tunnel, Norway. *Hydrogeol J* 8(5):480–493
- Kvæerner J, Snilsberg P (2011) Groundwater hydrology of boreal peatlands above a bedrock tunnel: drainage impacts and surface water groundwater interactions. *J Hydrol* 403(3):278–291
- Lei S (1999) An analytical solution for steady flow into a tunnel. *Ground Water* 37:23–26
- Liu XX, Shen SL, Xu YS, Yin ZY (2018) Analytical approach for time-dependent groundwater inflow into shield tunnel face in confined aquifer. *Int J Numer Anal Methods Geomech* 42:655–673
- Lyu HM, Sun WJ, Shen SL, Arulrajah A (2018) Flood risk assessment in metro systems of mega-cities using a GIS-based modeling approach. *Sci Total Environ* 626:1012–1025
- Ma L, Xu YS, Shen SL, Sun WJ (2014) Evaluation of the hydraulic conductivity of aquifers with piles. *Hydrogeol J* 22(2):371–382
- Malott S, O'Carroll DM, Robinson CE (2016) Dynamic groundwater flows and geochemistry in a sandy nearshore aquifer over a wave event. *Water Resour Res* 52(7):5248–5264
- Masset O (2011) Transient tunnel inflow and hydraulic conductivity of fractured crystalline rocks in the Central Alps (Switzerland). PhD Thesis, ETH, Zurich
- Molinero J, Samper J, Juanes R (2002) Numerical modelling of the transient hydrogeological response produced by tunnel construction in fractured bedrocks. *Eng Geol* 64(4):369–386
- Moon J, Fernandez G (2010) Effect of excavation-induced groundwater level drawdown on tunnel inflow in a jointed rock mass. *Eng Geol* 110(3–4):33–42

- Nash JE, Sutcliffe JE (1970) River flow forecasting through conceptual models, part I: a discussion of principles. *J Hydrol* 10(3):282–290
- Nikvar Hassani A, Katibeh H, Farhadian H (2016) Numerical analysis of steady-state groundwater inflow into Tabriz line 2 metro tunnel, northwestern Iran, with special consideration of model dimensions. *Bull Eng Geol Environ* 75(4):1617–1627
- Nikvar Hassani A, Farhadian H, Katibeh H (2018) A comparative study on evaluation of steady-state groundwater inflow into a circular shallow tunnel. *Tunnel Undergr Space Technol* 73:15–25
- Nilsen B, Palmström A (2001) Stability and water leakage of hard rock subsea tunnels. In: Adachi et al. (eds) *Proceedings of Conf. on Modern Tunneling Science and Technology*, Kyoto, Japan, 30 October–1 November 2001, pp 497–502
- Panthi KK, Nilsen B (2010) Uncertainty analysis for assessing leakage through water tunnels: a case from Nepal Himalaya. *Rock Mech Rock Eng* 43:629–639
- Ren QW, Dong YW, Yu TT (2009) Numerical modeling of concrete hydraulic fracturing with extended finite element method. *Sci Chin Ser E: Technol Sci* 52(3):559–565
- Rezaei M (2017) A new approach to water head estimation based on water inflow into the tunnel: case study—Karaj water conveyance tunnel. *Q J Eng Geol Hydrogeol* 50(2):126
- Rong Y, Xu XB, Cai XH (2006) Calculation of crack space and crack width of tunnel lining based on elastic foundation curved beam mode (in Chinese). *J Chongqing Jianzhu Univ* 28(5):23–26
- Russo SL, Gnani L, Peila D, Suozzi E (2013) Rough evaluation of the water-inflow discharge in abandoned mining tunnels using a simplified water balance model: the case of the Cogne iron mine (Aosta Valley, NW Italy). *Environ Earth Sci* 70:2753–2765
- Schleiss AJ (1997) Design of reinforced concrete linings of pressure tunnels and shafts. *Int J Hydropower Dams* 4(3):88–94
- Sefelnasr A, Gossel W, Wycisk P (2014) Three-dimensional groundwater flow modeling approach for the groundwater management options for the Dakhla Oasis, Western Desert, Egypt. *Environ Earth Sci* 72(4):1227–1241
- Sharifzadeh M, Karegar S, Ghorbani M (2013) Influence of rock mass properties on tunnel inflow using hydromechanical numerical study. *Arab J Geosci* 6(1):169–175
- Shin JH, Kim SH, Shin YS (2012) Long-term mechanical and hydraulic interaction and leakage evaluation of segmented tunnels. *Soils Found* 52(1):38–48
- Su K, Zhou Y, Wu H, Shi C, Zhou L (2017) An analytical method for groundwater inflow into a drained circular tunnel. *Ground Water* 55(5):712–721
- Wu YX, Shen SL, Yin ZY, Xu YS (2015a) Characteristics of groundwater seepage with cut-off wall in gravel aquifer, I: field observations. *Can Geotech J* 52(10):1526–1538
- Wu YX, Shen SL, Yin ZY, Xu YS (2015b) Characteristics of groundwater seepage with cut-off wall in gravel aquifer, II: numerical analysis. *Can Geotech J* 52(10):1539–1549
- Wu YX, Shen SL, Yuan DJ (2016) Characteristics of dewatering induced drawdown curve under blocking effect of retaining wall in aquifer. *J Hydrol* 539:554–566
- Wu YX, Shen JS, Chan WC, Hino T (2017) Semi-analytical solution to pumping test data with barrier, wellbore storage, and partial penetration effects. *Eng Geol* 226:44–51
- Xu YS, Ma L, Shen SL, Sun WJ (2012) Evaluation of land subsidence by considering underground structures that penetrate the aquifers of Shanghai, China. *Hydrogeol J* 20(8):1623–1634
- Yi ST, Hyun TY, Kim JK (2011) The effects of hydraulic pressure and crack width on water permeability of penetration crack-induced concrete. *Constr Build Mater* 25:2576–2583
- Zarei HR, Uromeihy A, Sharifzadeh M (2011) Evaluation of high local groundwater inflow to a rock tunnel by characterization of geological features. *Tunn Undergr Space Technol* 26:364–373
- Zhang W, Chen YC, Huang LC, Liu LJ (2015) 3D finite element analysis of seepage from a high pressure tunnel and study on its permeation stability (in Chinese). *J Water Resour Architect Eng* 13(5):212–217